Journal of Experimental Botany, Vol. 58, No. 14, pp. 3949–3960, 2007
doi:10.1093/jxb/erm249 Advance Access publication 17 November, 2007
This paper is available online free of all access charges (see http://jxb.oxfordjournals.org/open_access.html for further details)

Journal of Experimental Botany
www.jxb.oxfordjournals.org

RESEARCH PAPER

An extra-plastidial α-glucan, water dikinase from *Arabidopsis* phosphorylates amylopectin *in vitro* and is not necessary for transient starch degradation

Mikkel A. Glaring[1,*], Agnieszka Zygadlo[1,†], David Thorneycroft[3], Alexander Schulz[2], Steven M. Smith[3,4], Andreas Blennow[1] and Lone Baunsgaard[1,†]

[1] *Plant Biochemistry Laboratory, Center for Molecular Plant Physiology (PlaCe), Department of Plant Biology, Faculty of Life Sciences, University of Copenhagen, 40 Thorvaldsensvej, 1871 Frederiksberg C, Copenhagen, Denmark*

[2] *Plant Physiology and Anatomy Laboratory, Department of Plant Biology, Faculty of Life Sciences, University of Copenhagen, Denmark*

[3] *Institute of Molecular Plant Sciences, University of Edinburgh, Edinburgh EH9 3JH, UK*

[4] *ARC Centre of Excellence in Plant Energy Biology, University of Western Australia, WA 6009, Australia*

Received 18 July 2007; Revised 17 September 2007; Accepted 18 September 2007

Abstract

Starch phosphorylation catalysed by the α-glucan, water dikinases (GWD) has profound effects on starch degradation in plants. The *Arabidopsis thaliana* genome encodes three isoforms of GWD, two of which are localized in the chloroplast and are involved in the degradation of transient starch. The third isoform, termed AtGWD2 (At4g24450), was heterologously expressed and purified and shown to have a substrate preference similar to potato GWD. Analyses of *AtGWD2* null mutants did not reveal any differences in growth or starch and sugar levels, when compared to the wild type. Subcellular localization studies in *Arabidopsis* leaves and *in vitro* chloroplast import assays indicated that AtGWD2 was not targeted to the chloroplasts. The *AtGWD2* promoter showed a highly restricted pattern of activity, both spatially and temporally. High activity was observed in the companion cells of the phloem, with expression appearing just before the onset of senescence. Taken together, these data indicate that, although AtGWD2 is capable of phosphorylating α-glucans *in vitro*, it is not directly involved in transient starch degradation.

Key words: *Arabidopsis*, dikinase, GWD, phloem, starch degradation, starch phosphorylation.

Introduction

In recent years, significant progress has been made in elucidating the enzymatic pathways responsible for the degradation of transient starch in *Arabidopsis thaliana* (Lloyd *et al*., 2005; Smith *et al*., 2005; Zeeman *et al*., 2007). Analysis of plants mutated in plastidic glucan phosphorylase has suggested that the phosphorolytic pathway of starch degradation is not required under normal growth conditions (Zeeman *et al*., 2004). Rather, hydrolytic breakdown of starch leads to the formation of maltose and glucose as primary products of degradation (Niittylä *et al*., 2004; Weise *et al*., 2004). The analysis of starch degradation is confounded by the multitude of isoforms of enzymes capable of degrading starch or related glucans. Few studies of starch metabolism in *Arabidopsis* have focused on the function of starch-degrading enzymes not directly involved in the metabolism of transient starch or its degradation products. Many of these enzymes show subcellular localizations not compatible with a plastidic localization of starch and suggest alternative locations of starch or starch-like molecules. The *Arabidopsis* genome encodes two α-amylases and six β-amylases predicted to be localized outside the plastids (Lloyd *et al*., 2005). No *in vivo* substrate has so far been identified for any of these enzymes and there is little experimentally based information on their subcellular

* To whom correspondence should be addressed. E-mail: mig@life.ku.dk
† Present address: Aresa A/S, Symbion Science Park, 3 Fruebjergvej, 2100 Copenhagen Ø, Denmark.

localization. Mutations in the extra-plastidial isoform of β-amylase RAM1 (BAM5), which has been localized to the phloem (Wang *et al*., 1995), lead to a significant decrease in β-amylase activity in *Arabidopsis*, but only minor changes in starch metabolism (Laby *et al*., 2001; Kaplan and Guy, 2005).

The enzyme responsible for the initial attack on the granule has not been clearly identified, but contrary to previous beliefs, it has been determined that the endoamylolytic action of α-amylases is not solely responsible for this process (Kaplan and Guy, 2005; Yu *et al*., 2005). The production of maltose during the degradation of starch has implicated the β-amylases in starch degradation. β-amylases are exoamylases that produce maltose by successive cleavage from the non-reducing end. Furthermore, a recent report has provided evidence that the debranching enzyme (isoamylase) ISA3 acts directly at the granule surface in *Arabidopsis* (Delatte *et al*., 2006). This debranching activity presumably removes short branches from the granule surface enabling further degradation by the β-amylases. Based on these results, it was suggested that ISA3 and β-amylase act progressively to degrade the starch granule surface (Delatte *et al*., 2006). Suppression of a chloroplast-localized β-amylase in *Arabidopsis* (BAM3), and the corresponding potato orthologue, leads to a starch-excess phenotype in leaves as a result of impaired starch degradation (Scheidig *et al*., 2002; Kaplan and Guy, 2005). Maltose produced by β-amylase is exported from the chloroplast by the transporter MEX1 (Niittylä *et al*., 2004) and further metabolized in the cytosol by the glucanotransferase DPE2 (Chia *et al*., 2004; Lu and Sharkey, 2004). This process involves a recently identified cytosolic soluble heteroglycan (Fettke *et al*., 2005). This heteroglycan has been studied in *DPE2* mutants and found to be indirectly involved in starch degradation partly by acting as a carbohydrate acceptor for the DPE2-catalysed transfer of glucose from maltose (Fettke *et al*., 2006).

Regardless of the mechanism of soluble glucan release from the starch granule, it is clear that it requires the activity of the α-glucan, water dikinases (GWD, Lorberth *et al*., 1998; Yu *et al*., 2001; Ritte *et al*., 2002). The GWDs are responsible for phosphorylating the glycosyl residues of starch, a process that takes place during both biosynthesis and degradation (Nielsen *et al*., 1994; Ritte *et al*., 2004). Repressing or eliminating the activity of potato GWD or the *Arabidopsis* orthologue AtGWD1/SEX1 (At1g10760), leads to a severely reduced phosphate content in starch and a starch-excess phenotype in leaves caused by a decreased rate of starch degradation (Lorberth *et al*., 1998; Yu *et al*., 2001). One homologue of AtGWD1 in *Arabidopsis*, termed AtGWD3 or PWD (At5g26570), is chloroplastic and involved in the phosphorylation of pre-phosphorylated glucans, an activity which is essential for the complete degradation of transient starch during the night (Baunsgaard *et al*., 2005; Kötting *et al*., 2005). Despite the essential role of starch-bound phosphate in starch degradation, the link between phosphorylation and degradation is not understood. It has been suggested that the activity of amylolytic enzymes might rely on direct interaction with phosphate groups or that the inclusion of phosphate affects the properties of amylopectin (Blennow *et al*., 2002; Ritte *et al*., 2002). A recent report has shown that GWD activity stimulates the breakdown of starch granules *in vitro* by plastidial β-amylases, leading the authors to suggest that phosphorylation by GWD causes a partial unwinding of the amylopectin double helix, thereby facilitating a subsequent enzymatic attack (Edner *et al*., 2007).

A third GWD, named AtGWD2, with 50% homology to AtGWD1 has been identified in the *Arabidopsis* genome (Yu *et al*., 2001). AtGWD2 has a domain structure more similar to AtGWD1 than AtGWD3/PWD, but lacks an apparent chloroplast transit peptide, making it likely to be a cytosolic isoform of GWD. The putative extra-plastidial glucan phosphorylating activity raises some interesting questions about the function of AtGWD2 and prompted us to investigate the substrate preference of this enzyme and its involvement in transient starch metabolism.

Materials and methods

Plant material and growth conditions

The mutant *Atgwd2-1* was obtained by screening a T-DNA transformed *Arabidopsis* population from the University of Wisconsin Arabidopsis knockout facility (Krysan *et al*., 1999). *Atgwd2-2* was obtained directly from the GABI-Kat program (line 257E09; www.gabi-kat.de; Rosso *et al*., 2003). The mutant *Atgwd2-3* was obtained from the SALK T-DNA mutant population (line SALK_080260; Alonso *et al*., 2003) provided by the European *Arabidopsis* Stock Centre (NASC, http://arabidopsis.info). Homozygous mutants were isolated by PCR screening of isolated genomic DNA. Standard PCR conditions were used to amplify a section of DNA spanning the reported insertion site in *AtGWD2* (insert test primers for *Atgwd2-1*; GWDb3: AGAACTCTCCAAGAGATCTGTGGGC, GWDb4r: ATCTCTCAGCCTCTTTCTCTCGCTC, *Atgwd2-2*; GWDb10: GAGACTAACTATGGCACTTGTGGGT, GWDb11r: CCATTGACAGCAAAGACATGATGACC, *Atgwd2-3*; GWDb1: TACAGACCTCATGATGTTCAGTGGG, GWD2-12r: GATATTGCTCTCCCTTCCTTCGACT). Positives were verified by PCR using the insert test primers and primers matching the T-DNA border. Total RNA was isolated and reverse transcribed using standard molecular biology methods. The absence of a functional *AtGWD2* transcript was verified by PCR using the insert test primers and a positive control. The *Arabidopsis thaliana* ecotypes Columbia-0 and Wassilewskija and the *Atgwd2* mutants were grown from seed in potting compost in growth chambers at 20 °C and 70% relative humidity with an 8 h photoperiod at a photon flux density of 120 μmol photons m^{-2} s^{-1}.

Phylogenetic analysis

The phylogenetic tree was based on a previous version containing GWD sequences identified from higher plants (Baunsgaard *et al*., 2005). This tree was based on the alignment of the nucleotide

binding domains corresponding to amino acids 1006–1194 of AtGWD3. The tree was expanded by the addition of a new citrus homologue of AtGWD2 identified in HarvEST (unigene #16433, http://harvest.ucr.edu) and two pairs of poplar sequences of which one from each pair is represented in the phylogenetic tree (GWD3 clade: genome scaffold LG_II: 22.012.650-22.013.216 and GWD1 clade: LG_VIII: 12.855.187-12.856.452; http://www.jgi.doe.gov/poplar). Furthermore, sequences from organisms other than higher plants were included in the analysis. Three GWD homologues from the green alga *Chlamydomonas reinhardtii* were identified from a previously published phylogenetic analysis of GWDs [Mikkelsen *et al*., 2004; accession nos *Chlamydomonas* a, BG857380; b, BF866067/AW661031; c, genome release version 3.0, scaffold 32, 64268–65561 (http://genome.jgi-psf.org/Chlre3)]. Two GWDs from the green alga *Ostreococcus tauri* were identified in GenBank [accession nos AY570708 (spr1a) and AY570720 (spr1b)]. GWD homologues from the apicomplexan parasites *Cryptosporidium parvum* (mRNA sequence, accession no. XM_626438) and *Toxoplasma gondii* (assembled from EST accession nos BU575407, BG658300, BG659286, CN194874, and genomic sequence) were also included. Other accession numbers were as follows. AtGWD1 clade: AtGWD1, NP_563877; rice, AK103463; maize, AY109804; wheat, CAC22583; barley, BU993123; citrus, AAM18228; grape, EE077235; potato, Q9AWA5; tomato, BE435569; soybean, AW133227/BI945390; *Medicago*, CAE84830. AtGWD2 clade: AtGWD2, AAO42141. AtGWD3 clade: AtGWD3, AY747068; maize, AY108492; rice, AK072331; *Medicago*, BM779840. The alignment and the phylogenetic tree were created using the MEGA3 software available at www.megasoftware.net (Kumar *et al*., 2004).

Glucan-bound phosphate content

Glucose-6-phosphate and glucose-3-phosphate contents were determined by acid hydrolysis of glucan substrates followed by high-performance anion-exchange chromatography with pulsed amperometric detection (HPAEC-PAD) as previously described (Blennow *et al*., 1998). To minimize interference from incompletely hydrolysed glucans, samples were hydrolysed for 4 h. This minimizes, but does not eliminate, the content of maltose-6-phosphate which co-elutes with glucose-3-phosphate under the conditions used (Ritte *et al*., 2006). For the determination of C-6 to C-3 phosphorylation ratios, 0.5 ml fractions were collected and the incorporated label was measured by a liquid scintillation counter (1450 Microbeta, Perkin-Elmer).

Expression, purification and substrate specificity of AtGWD2

AtGWD2 was expressed in *Saccharomyces cerevisiae* as a C-terminal fusion to a V5 epitope and polyhistidine tag (6×His) and purified by affinity chromatography as previously described by Baunsgaard *et al*. (2005). The *waxy* maize amylopectin substrates were generated as described by Baunsgaard *et al*. (2005). Soluble starch from potato was obtained from Sigma-Aldrich (product number S 2004).

Autocatalytic phosphorylation and dikinase assays

For the determination of autocatalytic phosphorylation (autophosphorylation), a 10 μg sample of purified AtGWD2 was analysed as described by Mikkelsen *et al*. (2004). Dikinase activity assays were performed essentially as previously described by Mikkelsen *et al*. (2004). One microgram of purified AtGWD2 was incubated with 10 μM [β-^{33}P]ATP (150 000 dpm) and 5 mg ml^{-1} glucan substrate in a final volume of 100 μl (25 mM HEPES/KOH, pH 7.0, 10 mM NH_4Cl, 10 mM $MgCl_2$, 0.5 mM DTT, 0.2 mg ml^{-1} BSA). The reaction was incubated for 1 h at 30 °C and terminated by boiling. The polyglucan was precipitated with 1.8 ml 75% methanol/1% KCl and resuspended in 200 μl of water. This procedure was repeated four times and the final pellet was dissolved in 400 μl of water. Incorporation of labelled phosphate was determined by adding 3 ml scintillation liquid to the mixture and measuring the radioactivity with a liquid scintillation counter (1450 Microbeta, Perkin-Elmer). Initial enzyme kinetic studies using soluble potato starch as a substrate confirmed that the rate of phosphate incorporation was constant over the entire assay period and increased linearly with respect to enzyme concentration.

Expression analysis

For analysis of *AtGWD2* expression, a 1207 bp promoter fragment (primers GWDb1: 5' GAT GCA AAT TGT CTG CAG GGA AT; GWDFL: 5' GGC AGC TAT TCA TAA AAA AGA GGT AAC A, including an *attB1* and *attB2* site, respectively) was cloned in front of an enhanced green fluorescent protein (eGFP)-β-glucoronidase (GUS) fusion in the vector pKGWFS7 (Karimi *et al*., 2002) using the GATEWAY™ cloning technology (Invitrogen). The construct was transformed into *Agrobacterium* and introduced into *Arabidopsis thaliana* ecotype Columbia-0. After an initial screening of transgenic lines in the T_1 and T_2 generations, five lines were chosen for detailed analysis. GUS activity was determined by harvesting plant parts directly into an X-Gluc solution [1 mg ml^{-1} 5-bromo-4-chloro-3-indolyl β-D-glucuronide cyclohexylammonium salt (Duchefa Biochemie, The Netherlands), 10 mM titriplex III, 2 mM $K_3[Fe(CN)_6]$ and 2 mM $K_4[Fe(CN)_6]$ in a 0.1 M phosphate buffer pH 7.5], vacuum infiltrating for 30 min and incubating at 37 °C for 24 h. Stained material was subjected to a 20–50% ethanol series, fixed in FAA (50% ethanol, 5% formaldehyde, 10% acetic acid) for 30 min and subsequently destained with 70% ethanol before microscopy analysis.

GFP activity was investigated by confocal laser scanning microscopy as previously described by Baunsgaard *et al*. (2005). Staining for sieve-plates was performed by incubating thin strips of mature *Arabidopsis* leaves in a solution of analine blue for 30 min, followed by immediate inspection by confocal laser scanning microscopy (TCS SP2; Leica Microsystems, Wetzlar, Germany). A two-photon laser operating at 800 nm was used for excitation and emission was detected in the interval between 450 nm and 510 nm.

Subcellular localization

The entire ORF of AtGWD2 as well as a fragment containing the 158 N-terminal amino acids was fused to enhanced GFP (eGFP) behind the constitutive 35S promoter in the binary vector pK7FWG2 (Karimi *et al*., 2002) using the GATEWAY™ cloning technology (Invitrogen). The constructs were introduced into *Arabidopsis thaliana* ecotype Columbia-0. For tobacco transient expression, fragments of AtGWD2 were PCR amplified using uracil-containing primers and cloned into the vector pPS48uYFP using an improved USER™ (uracil-specific excision reagent, New England Biolabs) cloning procedure (Nour-Eldin *et al*., 2006). The transit peptide of AtGWD1 was fused to AtGWD2 by simultaneous cloning of both fragments. The constructs were transformed into *Agrobacterium* and transiently expressed by infiltration in *Nicotiana benthamiana* as previously described by Voinnet *et al*. (2003). All constructs were analysed by a confocal laser scanning microscope (TCS SP2; Leica Microsystems, Wetzlar, Germany) equipped with a 20×/0.70 or 63×/1.20 PL APO water immersion objective. A 488 nm laser line was used for excitation and emission was detected between 510 nm and 535 nm for GFP fluorescence, 520 nm and 550 nm for YFP fluorescence, and 650 nm and 750 nm for chlorophyll autofluorescence.

In vitro *import assays*

Constructs containing *AtGWD2* alone and *AtGWD2* fused to the predicted transit peptide of *AtGWD1* were cloned in the vector

pGEM-4Z (Promega GmbH, Mannheim, Germany) and transcribed *in vitro* using SP6 RNA polymerase. Products were translated *in vitro* in the presence of [^{3}H]leucine using a Rabbit Reticulocyte Lysate system (Promega GmbH, Mannheim, Germany) according to the manufacturer's instructions. Intact chloroplasts were isolated from pea seedlings (*Pisum sativum*, var. Kelvedon Wonder) and *in vitro* import assays were carried out as reported by Robinson and Mant (2002). Samples were analysed by SDS-PAGE and autoradiography.

Electron microscopy

Inflorescence segments were cut from *Arabidopsis* wild-type Columbia-0 and the mutant *Atgwd2-2*. Fixation, staining, and image acquisition was performed as previously described by Schulz *et al.* (1998).

Results

The AtGWD2 homologue

A cDNA encoding AtGWD2 was obtained from the RIKEN *Arabidopsis* full-length (RAFL) cDNA collection (GenBank accession no. BT004118). This clone included the entire 1278 amino acids open reading frame (ORF) plus 5' and 3' untranslated regions. It is encoded by a 7.4 kb locus on chromosome 4 divided into 32 exons (At4g24450). The ORF includes the conserved phosphohistidine and nucleotide binding domains in the C-terminal end and the tandem repeated starch binding domains in the N-terminal end, similar to those present in AtGWD1 and potato GWD (Yu *et al*., 2001; Mikkelsen *et al*., 2006). The starch binding domain from potato GWD has been shown to bind to granular starch *in vitro* and this type of domain appears to be specific for enzymes involved in plastidial starch metabolism (Mikkelsen *et al*., 2006). Alignment of the conserved tryptophanes in the starch binding domains (Mikkelsen *et al*., 2006) showed that AtGWD2 lacks 78 amino acids in the N-terminal, when compared to AtGWD1. This truncation covers the entire predicted transit peptide of AtGWD1. Prediction of putative subcellular location by Predotar (http://urgi.versailles.inra.fr/predotar; Small *et al*., 2004) and TargetP (www.cbs.dtu.dk/services/TargetP; Emanuelsson *et al*., 2000) did not indicate the presence of a transit peptide. Together these observations suggest that AtGWD2 is a non-plastidic paralogue of AtGWD1.

Available sequence databases were analysed in an effort to identify putative orthologues of *AtGWD2* in other plants. Numerous homologous sequences were identified among ESTs and genomic survey sequences from *Brassica napus*, *Brassica rapa*, and *Brassica oleracea*, although none of these sequences (either singly or assembled) covered the entire nucleotide binding domain used in previous phylogenetic studies of GWDs (Baunsgaard *et al*., 2005). The sequence identity to *AtGWD2* was generally high, usually around 70–90% at both the nucleotide and protein levels depending on the sequence region. An EST clone from the bark of *Poncirus trifoliata* was identified in GenBank (accession nos CV711759 and CV711760). The clone belongs to a unigene cluster assembled from four sequences from *Poncirus trifoliata* (2), *Citrus clementina* (1), and *Citrus sinensis* (1) in the HarvEST project (http://harvest.ucr.edu). The sequence matches the 475 C-terminal amino acids of AtGWD2 and shows 68% identity and 82% similarity at the protein level. Intriguingly, this clone is the only indication of the existence of GWD2 orthologues outside the Brassicaceae family, to which *Arabidopsis* belongs. The poplar genome contained four GWD homologues, represented as pairs of closely related sequences, but no homologues of *AtGWD2*. A search of the rice genome revealed two sequences similar to *AtGWD1* and *AtGWD3/PWD* from *Arabidopsis*. No sequence with significant homology to *AtGWD2* was present, indicating that the monocot rice does not contain this isoform.

The phylogenetic study of higher plant GWDs previously reported (Baunsgaard *et al*., 2005) was expanded by including newly identified sequences from higher plants, the apicomplexan parasites *Cryptosporidium parvum* and *Toxoplasma gondii* and sequences from the green algae *Chlamydomonas reinhardtii* and *Ostreococcus tauri*. The phylogenetic tree showed two groups of GWDs comprising the orthologues of AtGWD1 and AtGWD3/PWD from higher plants (Fig. 1). The two representatives of GWD2 formed a group closely related to the GWD1 sequences, clearly demonstrating their relationship with the GWD1 group.

Expression and purification of AtGWD2

A fusion protein consisting of AtGWD2 and a C-terminal V5 epitope and polyhistidine tag (6×His) was heterologously expressed in *Saccharomyces cerevisiae* and purified to apparent homogeneity using affinity chromatography. The identity of the fusion protein was confirmed by SDS-PAGE and immunoblotting using an anti-V5 antibody. Enzyme activity was verified by autophosphorylation of the purified protein following incubation with [β-^{33}P]ATP. Autophosphorylation is the first step in the dikinase reaction mechanism. It results in a stable phosphorylated intermediate and the step can be completed in the absence of a glucan substrate (Ritte *et al*., 2002; Mikkelsen *et al*., 2004). Separation of the labelled products by SDS-PAGE and visualization by autoradiography revealed that AtGWD2 was significantly labelled by this procedure (Fig. 2).

Substrate specificity of AtGWD2

The *in vitro* substrate specificity of purified AtGWD2 was investigated using a series of enzymatically modified substrates previously used to characterize the AtGWD3 enzyme (Baunsgaard *et al*., 2005). These substrates were

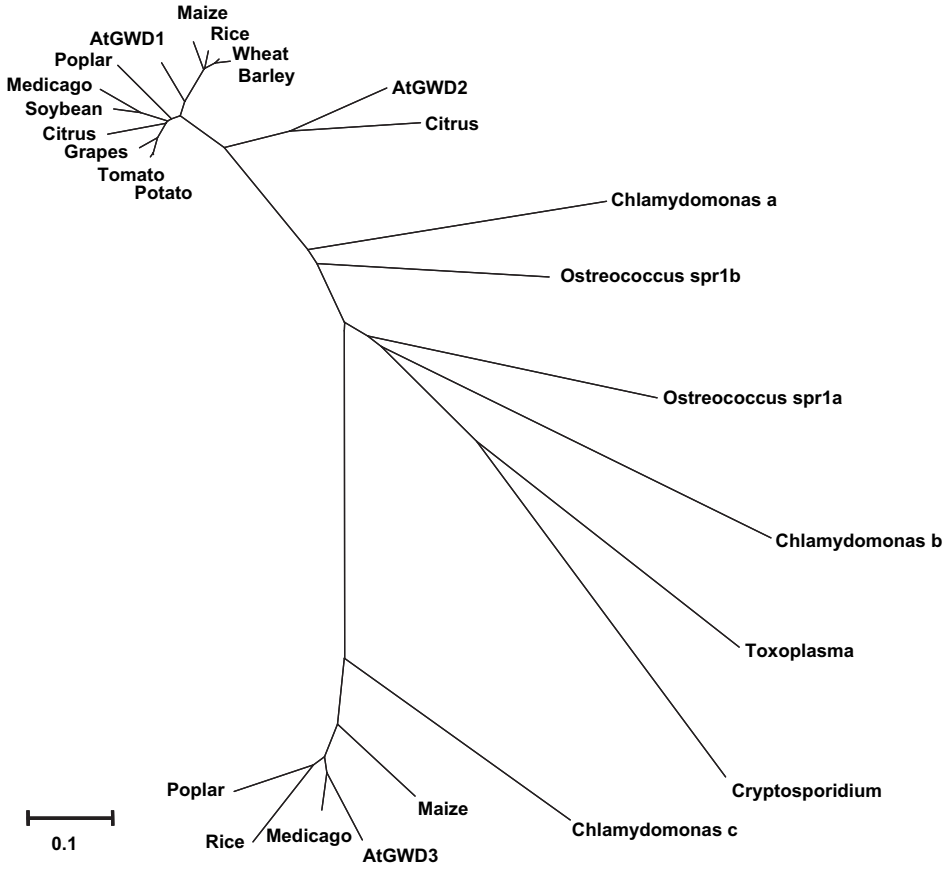

Fig. 1. A phylogenetic tree of the nucleotide binding domain of GWD sequences from selected organisms. The tree was constructed on the basis of available protein sequences or translated genome sequences and expressed sequence tags. The alignment was created and visualized using the MEGA3 software (Kumar *et al*., 2004). Accession numbers are given in the Materials and methods. The scale indicates the average substitutions per site.

based on *waxy* maize amylopectin, which has a very low natural level of covalently linked phosphate-groups. Three modified substrates were generated: (i) *waxy* maize amylopectin elongated by phosphorylase *a*, (ii) *waxy* maize amylopectin pre-phosphorylated with purified potato GWD, and (iii) elongated and pre-phosphorylated *waxy* maize amylopectin. Purified AtGWD2 was incubated with [β-^{33}P]ATP and the maize glucan substrates and the efficiency of glucan phosphorylation was determined by measuring the amount of incorporated label (Table 1). Minimal activity was detected on glycogen (data not shown), the unmodified amylopectin, and the pre-phosphorylated amylopectin. Elongating the amylopectin substrate led to a large increase in specific activity and pre-phosphorylation further increased this activity. Maximum activity was obtained on a soluble starch from potato. Soluble potato starch has previously been used as a substrate for determining starch-phosphorylating enzyme activity in plant extracts (Ritte *et al*., 2003). The substrate specificity of AtGWD2 thus resembles the results obtained for potato GWD (Ritte *et al*., 2002; Mikkelsen *et al*., 2004) and the activity is not dependent on previous

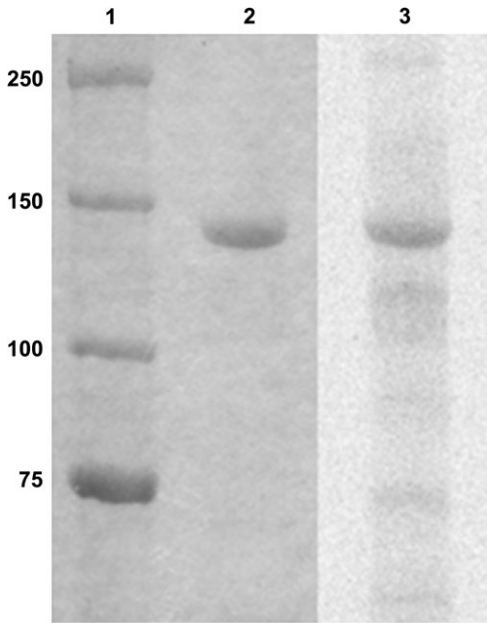

Fig. 2. Autophosphorylation of purified AtGWD2. (1) Marker. (2) Purified AtGWD2 incubated with [β-^{33}P]ATP, separated by SDS-PAGE and stained with Coomassie Brilliant Blue. (3) Autoradiogram of lane 2.

Table 1. *Activity of purified AtGWD2 on various glucan substrates*

Substrate	Mean chain length (DP)[c]	Phosphate content[a, c]	Specific activity (mU mg^{-1} protein)[b]
Amylopectin	23.5	0.1	0.02±0.01
Amylopectin, pre-phosphorylated	24.8	0.5	0.04±0.01
Amylopectin, elongated	29.7	0.1	0.49±0.02
Amylopectin, elongated and pre-phosphorylated	30.8	39.4	0.65±0.18
Soluble starch	ND	ND	1.36±0.21

[a] nmol glucose-6-phosphate mg^{-1} starch.
[b] 1 unit (U) is defined as 1 μmol phosphate incorporated min^{-1} at 30 °C.
[c] Values for mean chain length and glucose-6-phosphate content were obtained from Baunsgaard *et al.* (2005). Standard deviations from three activity experiments are given in parenthesis. ND, not determined.

phosphorylation, as has been reported for AtGWD3/PWD (Baunsgaard *et al*., 2005; Kötting *et al*., 2005).

The ratio between C-6 and C-3 phosphorylation was determined by acid hydrolysis of labelled soluble starch and separation by high-performance anion-exchange chromatography (HPAEC). Fractions collected from the peaks corresponding to glucose-6-phosphate and glucose-3-phosphate were labelled at a ratio of 86:14. It has recently been determined that phosphorylation of the C-6 and C-3 position is selectively catalysed by the GWD1 and GWD3/PWD isoforms, respectively (Ritte *et al*., 2006). The obtained ratio shows that AtGWD2 primarily phosphorylates the C-6 position. Since maltose-6-phosphate, which is formed as a result of incomplete hydrolysis, has been shown to co-elute with glucose-3-phosphate under the conditions used, it is likely that AtGWD2 exclusively phosphorylates the C-6 position as has been observed for both AtGWD1 and potato GWD (Ritte *et al*., 2006).

Characterization of AtGWD2 *mutants*

Three T-DNA insertion mutants in the *AtGWD2* gene were isolated from two different ecotype backgrounds. An insertion in the ecotype Wassilewskija was obtained by screening a T-DNA transformed *Arabidopsis* population from the University of Wisconsin *Arabidopsis* knockout facility (Krysan *et al*., 1999). The insertion was mapped to exon 9 and the mutant line called *gwd2-1*. Two mutants in the Columbia (Col-0) background were identified from flanking sequence tags (FSTs). A mutant with the insert mapped to exon 15 was obtained from the GABI-Kat collection (Rosso *et al*., 2003) and a mutant with an insertion in exon 23 was obtained from the SALK collection (Alonso *et al*., 2003). These lines were named *Atgwd2-2* and *Atgwd2-3*, respectively. Homozygous lines were selected by PCR screening of genomic DNA and insertions were verified by PCR using primers matching the borders of the T-DNA insert and the *AtGWD2* gene. Reverse transcription (RT)-PCR analysis confirmed that none of the mutants produced a functional *AtGWD2* transcript. Plants were grown for at least three generations with no visible phenotype from an observation of growth and development when compared with the wild type. Iodine staining of leaves after the dark period did not reveal any accumulation of starch in the mutants. Enzymatic determination of starch and sugar content (glucose, fructose, and sucrose) in leaves after both the light and dark periods did not reveal any differences when compared with the wild type. In contrast to the results obtained with null mutants of *AtGWD1* and *AtGWD3/PWD* (Yu *et al*., 2001; Baunsgaard *et al*., 2005; Kötting *et al*., 2005), null mutants of *AtGWD2* do not appear to be affected in degradation of transient starch under standard growth conditions.

AtGWD2 *is expressed in the companion cells of the phloem in an age-dependent manner*

Studies on the frequency and distribution of ESTs in tissues of *Arabidopsis* suggested that *AtGWD2* is expressed late in the plant life cycle. Two ESTs were isolated from a leaf senescence library (GenBank accession nos CD529796 and CD529114) and a further two were isolated from flower or silique libraries (GenBank accession nos AV564246 and AU227674). In order to investigate the precise expression pattern of *AtGWD2*, a 1207 bp promoter fragment, corresponding to the entire genomic region from the end of the upstream ORF (At4g24440) to the start codon of *AtGWD2*, was cloned in front of an enhanced green fluorescent protein-β-glucoronidase fusion (GFP-GUS). This promoter region included the 5' untranslated region, containing exon 1 and part of exon 2. The promoter construct was transformed into *Arabidopsis* wild type and the T_3 and T_4 generations were analysed by X-Gluc staining for GUS activity. A highly restricted pattern of expression was observed with strong expression in the vascular tissues of leaves, stem, roots, flowers, and siliques (Fig. 3). This vascular expression pattern was highly age-dependent in all tissues, appearing just before the onset of senescence. The first signs of GUS activity in developing *Arabidopsis* plants were seen in the cotyledons of approximately 3-week-old plants (grown in 8 h light) immediately prior to the first visible signs of senescence (i.e. yellowing). The appearance of GUS activity during development of the rosette followed this pattern, with activity appearing in the lower leaf-pairs before visible senescence symptoms were observed (Fig. 3B). At the time of emergence of the inflorescence, GUS activity could be detected in the majority of mature leaves. This age-related pattern was repeated in developing flowers and siliques (Fig. 3C–F). Activity in flowers was observed in the sepals and stamens after flower opening (Fig. 3D) and strong activity was detected in the floral organ abscission zone (Fig. 3F).

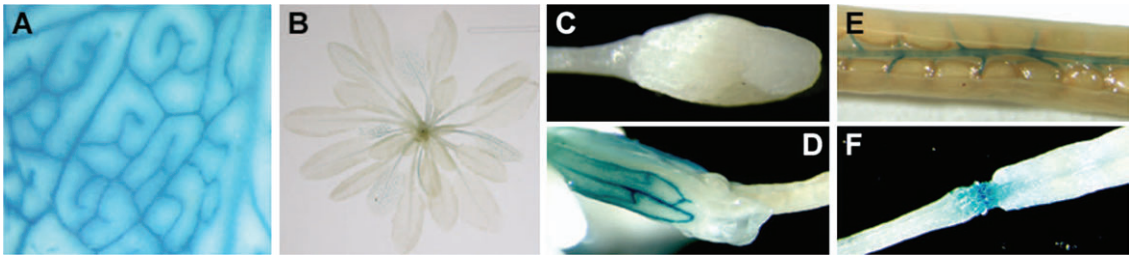

Fig. 3. GUS staining of *Arabidopsis* plants expressing a GFP-GUS fusion from the *AtGWD2* promoter. (A) A mature rosette leaf showing the vascular expression pattern. (B) A 7-week-old *Arabidopsis* plant showing expression in the lower leaf pairs. (C) Immature flower bud. (D) Mature flower with emerging silique. GUS activity can be observed in the sepals. (E) Maturing silique showing activity in the dehiscence zone between the silique walls. (F) Activity in the floral organ abscission zone after senescence of the flower and formation of the silique.

The emerging siliques retained the staining in the abscission zone during development. During silique maturation, activity appeared in the dehiscence zone between the silique walls (Fig. 3E) and in the vascular tissues of the silique walls. Cross-sections of mature leaves localized the GUS signal to the abaxial (lower) side of the primary vascular bundle, coincident with the location of the phloem (data not shown). The tissue specificity and developmental pattern of *AtGWD2* promoter activity were compared to the microarray data collected in Genevestigator (www.genevestigator.ethz.ch; Zimmermann *et al*., 2004). The analysis revealed high levels of *AtGWD2* expression in senescent leaves, cauline leaves, siliques, and mature flower parts, in good agreement with the observed GUS activity pattern.

The GFP-GUS fusion expressed from the *AtGWD2* promoter was used to locate the specific cell types in which the *AtGWD2* promoter was active. Mature leaves of bolting plants were investigated by confocal laser scanning microscopy (CLSM). GFP fluorescence was observed in long narrow cells in the vascular bundles (Fig. 4A). These cells contained both vacuoles and chloroplasts (Fig. 4B). The presence of chloroplasts indicated that these cells were either phloem parenchyma cells or companion cells. To verify their identity, phloem sieve-plates were stained with aniline blue and their location was investigated by CLSM. Sieve-plates were observed adjacent to the GFP-labelled cells in optical cross-sections and were close to the junction between two labelled cells (Fig. 4B, inset). This confirmed the identity of the GFP-labelled cells as phloem companion cells.

AtGWD2 is not targeted to the chloroplast

As mentioned above, analysis of putative transit peptide sequences in AtGWD2 indicated that the enzyme is an extra-plastidial isoform of GWD. To determine the subcellular localization of AtGWD2, two fusions to GFP were constructed. The first construct contained the full-length AtGWD2 protein, while the second construct included the 158 N-terminal amino acids. Expression of the fusion proteins was driven by the 35S promoter. The

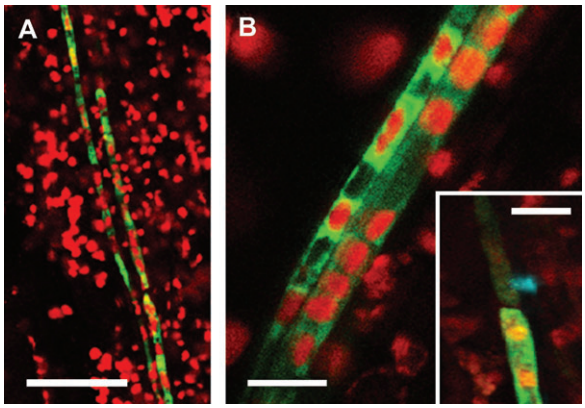

Fig. 4. Localization of the GFP-GUS fusion expressed from the *AtGWD2* promoter. (A) GFP fluorescence (green) in long narrow cells of a vascular bundle. Scale bar 40 μm. (B) Closer view of the fluorescent cells, showing chloroplasts (red) and putative vacuoles (dark 'holes'). (B, inset) Aniline blue staining of a sieve-plate (light blue) in an adjacent sieve element. Scale bar 10 μm.

full-length fusion was analysed by transient expression in onion epidermis and stable transformation of *Arabidopsis*. None of these approaches gave any visible GFP signal by either conventional fluorescence microscopy or CLSM. However, the AtGWD2 (aa1–158)-GFP fusion protein gave rise to clear fluorescence in several transgenic *Arabidopsis* lines when viewed with CLSM. The fluorescence was primarily restricted to the epidermal cell layer and the GFP signal was present in the nucleus and in a narrow band along the cell wall (Fig. 5A). This pattern coincides with that of free GFP (Haseloff *et al*., 1997) and suggests a cytoplasmic localization of the fusion protein. Analysis of guard cells showed clear GFP activity outside the chloroplasts (Fig. 5B), supporting the results of the transit peptide predictions.

As a second approach, full-length AtGWD2 and a series of three C-terminally truncated versions (carrying N-terminal fragments including 610, 158, and 61 amino acids, respectively) were fused to YFP and examined using a tobacco transient expression system. The two fusions containing the full-length AtGWD2 and 610 N-terminal amino acids did not give rise to any visible

fluorescence, similar to what was observed for the full-length fusion in *Arabidopsis*. The 158 and 61 amino acids fusions showed identical localization patterns with clear fluorescence in both epidermal and mesophyll cells. In epidermal cells the YFP signal was similar to the GFP signal observed in *Arabidopsis*, with fluorescence along the cell wall and in the nucleus (data not shown). In mesophyll cells the signal was clearly located outside the chloroplasts (Fig. 5D). N-terminal addition of the 78 amino acids predicted transit peptide from AtGWD1 targeted both fusions to the chloroplasts in tobacco cells. The chloroplast targeted fusion protein carrying the 158 N-terminal amino acids of AtGWD2 was located at the surface of rounded structures, presumed to be starch granules, inside the chloroplasts (Fig. 5C). This fusion protein contains one of the N-terminal starch binding domains of AtGWD2 and the binding indicates that this domain is functional *in vivo*. To verify that the cytoplasmic localization was not simply due to the loss of N-terminal targeting information caused by proteolytic breakdown of the fusion protein, western blotting was performed using a GFP-antibody. Both fusions gave a strong band of the correct size, with only a minor breakdown product in the AtGWD2 (aa1–158)-GFP fusion (Fig. 5E).

To corroborate the results of the AtGWD2-GFP/YFP fusion experiments, chloroplast import studies were performed to examine the localization of AtGWD2. Full-length AtGWD2 was transcribed and translated in the presence of radiolabelled [^{3}H]leucine *in vitro* and incubated with intact chloroplasts (C) isolated from pea seedlings. After incubation, the chloroplasts were treated with thermolysine (C+) which degrades the non-imported precursor proteins leaving the chloroplast structure intact. Chloroplasts were then fractionated into a stromal fraction (S) and a thylakoid membrane fraction (T). Fractions were loaded onto a SDS-PAGE gel and subjected to autoradiography. The resulting autoradiogram showed that the AtGWD2 protein (Fig. 6; GWD2 panel, lane C) was completely degraded by thermolysine treatment after incubation with intact chloroplasts (Fig. 6; GWD2 panel, lane C+) suggesting that AtGWD2 does not contain an *in vitro* functional transit peptide allowing import into the chloroplast. In contrast to these results, a control construct with the AtGWD1 transit peptide fused to the N-terminus of AtGWD2 was *in vitro* imported and gave a labelled double band around the correct size (~150 kDa) in the intact chloroplast preparations (Fig. 6; TP-GWD2 panel, lanes C and C+) and in the stroma (Fig. 6; TP-GWD2 panel, lane S). The double band may be due to a plastidic proteolytic activity acting on the imported translation product or alternatively, a post-translational modification of the protein. Compared with the unmodified AtGWD2, the fusion products were protected from thermolysine

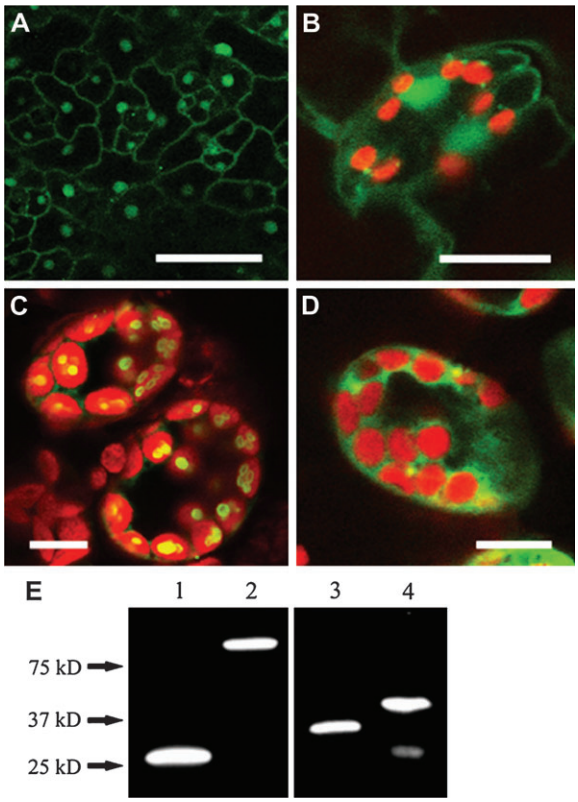

Fig. 5. Localization of fusion proteins between AtGWD2 and GFP/YFP. (A) *Arabidopsis* expressing the AtGWD2 (aa1–158)-GFP fusion in epidermal cells. GFP fluorescence (green) can be observed along the cell walls and in the nuclei. (B) An *Arabidopsis* guard cell pair. The fusion protein does not co-localize with the chloroplasts (red). (C, D) Tobacco mesophyll cells transiently expressing the AtGWD2 (aa1–158)-YFP fusion with (C) or without (D) the AtGWD1 transit peptide. Scale bars: (A) 50 μm; (B, C, D) 10 μm. (E) Western blot of the fusion proteins expressed in tobacco using a GFP antibody. Expression controls with free GFP (1) and a GFP-GUS fusion (2) driven by the 35S promoter. C-terminal YFP fusion proteins containing 61 amino acids (3) or 158 amino acids (4) of the AtGWD2 N-terminal end.

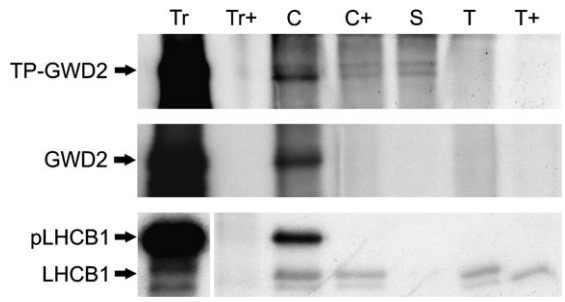

Fig. 6. Chloroplast import assays on native AtGWD2 and AtGWD2 fused to the transit peptide of AtGWD1 (TP-GWD2). Constructs were transcribed and translated *in vitro* in the presence of [^{3}H]leucine and subsequently incubated with isolated intact pea chloroplasts. The LHCB1 protein (light-harvesting chlorophyll *b* binding protein, thylakoid membrane protein) was used as an import control. The lanes correspond to *in vitro*-translated precursor (Tr), thermolysine-treated precursor (Tr+), total, washed chloroplasts immediately after import (C), thermolysine-treated chloroplasts (C+), stromal extract (S), isolated thylakoids (T), trypsin-treated thylakoids (T+).

digestion after incubation with intact chloroplasts (Fig. 6; TP-GWD2 panel, lane C+) indicating that TP-AtGWD2 was translocated into the chloroplast. The nuclear-encoded LHCB1 protein (light-harvesting chlorophyll *b* binding protein), which is targeted to the thylakoid membranes, was used as a control of the chloroplast import assay (Fig. 6; LHCB1 panel, lanes T and T+).

Sieve element starch in Arabidopsis

The specific expression of *AtGWD2* in the companion cells of the phloem prompted an investigation of the presence of starch in sieve element plastids of *Arabidopsis*. Plastids are a universal feature of sieve elements and are characterized by various types of inclusions, including starch granules (van Bel *et al*., 2002). The function of the sieve element plastids in phloem translocation is not known, but it has been suggested that they might serve as storage units, provided that the enzymes needed for biosynthesis and degradation of the included macromolecules are present (van Bel *et al*., 2002). Sieve element starch has previously been observed in the root protophloem of *Arabidopsis* (Wu and Zheng, 2003).

Electron microscopy (EM) was used to investigate the appearance of sieve element starch granules in *Arabidopsis* wild-type Columbia-0 and the mutant *Atgwd2-2*. Sections of the inflorescence stem showed sieve element plastids containing round starch granules with a diameter of approximately 200–300 nm (Fig. 7). Most plastids were surrounded by a seemingly intact double membrane. No differences were observed between wild type and mutant, with respect to size and morphology of starch granules (data not shown). However, the EM micrographs were not generally suitable for total quantification of sieve element starch.

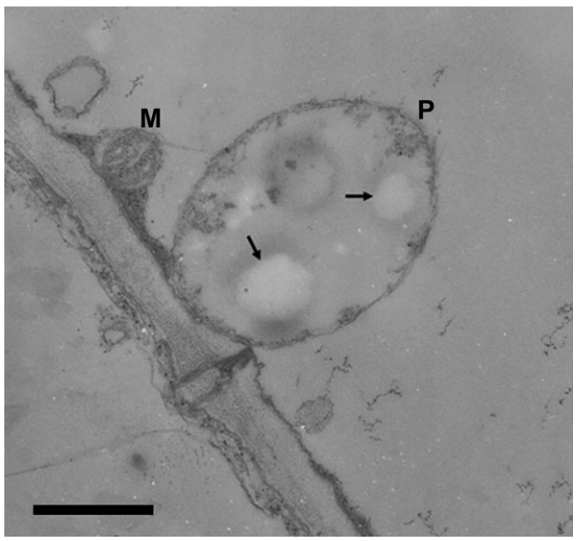

Fig. 7. Electron microscopy image of a sieve element plastid from the inflorescence of *Arabidopsis*. M, mitochondrion. P, plastid. Arrows indicate starch granules. Scale bar 500 nm.

Discussion

A search of available sequence data from higher plants revealed homologues of *AtGWD2* in three *Brassica* species and in a collection of *Citrus* sequences. This restricted pattern of appearance is intriguing as homologues of both *AtGWD1* and *AtGWD3/PWD* can be readily identified in most higher plants (Baunsgaard *et al*., 2005). The apparent lack of homologues of *AtGWD2* among the abundance of ESTs and genomic sequences from monocot species, suggests that *AtGWD2* evolved after the divergence of the monocots and dicots. The phylogenetic tree shows that the GWD2 sequences form a group separate from the GWD1 orthologues of both monocots and dicots. This suggests a duplication of GWD before the divergence of monocots and dicots, although this does not take into account differences in evolutionary rate caused by varying selective pressure. Another, perhaps more unlikely, explanation is that the monocots have lost the gene corresponding to *AtGWD2* during the course of evolution. The continuous release of new sequence data from many plants species is likely to shed more light on this question in the future.

In vitro analysis of purified enzyme demonstrated that AtGWD2 was active on elongated glucan chains and did not require previous phosphorylation of the substrate. This substrate preference resembles that of potato GWD (Ritte *et al*., 2002; Mikkelsen *et al*., 2004). Furthermore, AtGWD2 primarily phosphorylated the C-6 position of the glycosyl residues. These results, along with the data that indicate that AtGWD2 is an extra-plastidial enzyme, support the idea that AtGWD2 is an active cytosolic isoform of AtGWD1. Analysis of *Arabidopsis* mutants demonstrated that the enzyme is not required for the degradation of transient starch, suggesting that AtGWD2 is active on an, as yet unidentified, glucan substrate.

AtGWD2 promoter activity was restricted to the companion cells of the phloem and was highly age-dependent. The expression followed the development of senescence in leaves, flowers, and siliques and was usually observed just before the appearance of visible senescence symptoms. The link with senescence suggests that the AtGWD2 enzyme might be involved in the breakdown of starch or starch-like structures during the withdrawal of nutrients from the senescing leaf. The specific expression in companion cells could implicate AtGWD2 in either the transport of carbohydrates through the phloem or in the degradation of phloem-specific structures. Presently, there is no specific evidence for the existence of large α-linked polysaccharides, other than starch, in phloem tissues. It is possible that the cytosolic soluble heteroglycan that has

been identified in *Arabidopsis* (Fettke *et al*., 2005) is also present in companion cells and phloem parenchyma cells, but there is no evidence to suggest that α-glucan, water dikinase activity would be required for its metabolism.

The observation that the major form of β-amylase in *Arabidopsis* is localized in the phloem sieve elements lead to the idea that β-amylase activity might play a role in preventing build-up of polymerized polysaccharides that would impede flow through the sieve-plates (Wang *et al*., 1995). Given the location of AtGWD2 and the RAM1 β-amylase in *Arabidopsis* it is tempting to speculate that they might function in the metabolism of larger polysaccharides in the phloem sieve elements, either as a way of preventing their build-up or as a way of regulating the transport and availability of sugars. Proteins present in sieve elements are synthesized in companion cells and transferred via plasmodesmata. The size of the AtGWD2 protein would most likely prevent non-specific (passive) trafficking between these two cell types (Lough and Lucas, 2006), but experiments with *Cucurbita maxima* have shown that phloem exudate contains proteins ranging in molecular weight from 10–200 kDa (Balachandran *et al*., 1997). How this specific (selective) trafficking of proteins destined for the sieve element is accomplished is unknown. Many phloem proteins can modify the size exclusion limit of mesophyll plasmodesmata enabling transport of larger proteins and compounds (Balachandran *et al*., 1997). There is also good evidence to suggest that selective trafficking can be mediated by chaperones or shuttle-proteins that target the selected proteins to the plasmodesmal channel (Lee *et al*., 2003). Furthermore, transport of the encoding mRNA to the sieve element has been described for a number of proteins, among them the sucrose transporter SUT1 from potato (Lough and Lucas, 2006). The SUT1 protein is present in sieve elements, but transcription occurs in companion cells and the mRNA is found in both cell types (Kühn *et al*., 1997). Whether the transported mRNA gives rise to any protein in the sieve element is still unresolved. Although these data show that the *AtGWD2* promoter is active in companion cells, a sensitive anti-AtGWD2 antibody would be required to analyse whether or not the protein itself resides in sieve elements where RAM1 has been localized (Wang *et al*., 1995). The lack of any clear phenotype in null mutants of *AtGWD2* and *RAM1* (Laby *et al*., 2001) suggests that their contribution to sugar metabolism under normal circumstances is minor. The expression of *RAM1* is heavily upregulated in response to sucrose, indicating that sucrose affects the amount of RAM1 substrate (Mita *et al*., 1995). Induction of *AtGWD2* promoter activity has been observed in seedlings germinated on sucrose-containing media, suggesting a similar response of *AtGWD2* (data not shown).

Both GWD and isoamylase sequences have been proposed to be a prerequisite for the appearance of semi-crystalline starch-like polymers (Coppin *et al*., 2005), since these enzymes distinguish plant starch metabolism from the glycogen metabolism of animals, fungi, and bacteria. The presence of *GWD*s appears to be a ubiquitous feature of all organisms accumulating semi-crystalline storage polysaccharides. Homologues of *GWD* can be found in plants, the green and red algae, and in apicomplexan parasites (Mikkelsen *et al*., 2004; Ral *et al*., 2004; Coppin *et al*., 2005). If the existence of GWDs is a prerequisite for the successful metabolism of semi-crystalline polysaccharides, it is tempting to assume that AtGWD2 acts on such a substrate *in vivo*. The starch granules in the plastids of *Arabidopsis* phloem sieve elements present an appealing target for the action of AtGWD2. It has been determined that sieve element starch in bean hypocotyls contains a high proportion of α-1,6 linkages and is structurally distinct from ordinary starch (Palevitz and Newcomb, 1970). The sieve element plastid membrane degrades during development of root protophloem in *Arabidopsis* leaving starch granules free in the lumen (Wu and Zheng, 2003). Older sieve elements in bean also contain starch granules free in the lumen, but the authors could not conclude whether they were released naturally during ageing or the result of cutting and fixing the tissue (Palevitz and Newcomb, 1970). Pressure release in fava bean sieve elements leads to immediate rupture of the plastids. It was speculated that the liberated contents of the sieve element plastids, including the starch granules, might aid in plugging the sieve pore in response to wounding (Knoblauch and van Bel, 1998). The apparent lack of a chloroplast transit peptide and the late expression in the plant life cycle could suggest that AtGWD2 acts on starch granules released from degrading plastids in ageing plants. The structure of sieve element plastids in the inflorescence stem of *Arabidopsis* was investigated. Although the plastids were still surrounded by an apparently intact double membrane, the nature and integrity of this membrane is unknown. Starch granules were present in both wild type and an *Atgwd2* mutant, but because the plane of sectioning in EM does not necessarily pass through the centre of the granule, quantification of the results can be difficult. Detecting any differences in the number or size distribution of sieve element starch granules in wild type and mutant would require a more comprehensive quantitative survey. It is worth noting that many plant species, particularly among the monocots, do not contain starch in the sieve element plastids (Behnke, 2003).

Acknowledgements

We thank Lis B Møller, Per Lassen Nielsen, and Lise Girsel for technical assistance and René Mikkelsen for valuable advice and discussions. RIKEN Genomic Sciences Center is gratefully acknowledged for providing the AtGWD2 full-length cDNA clone. This

project was supported by a grant from The Danish Research Council for Technology and Production Sciences (Grant no. 23-04-0239).

References

Alonso JM, Stepanova AN, Leisse TJ, *et al.* 2003. Genome-wide insertional mutagenesis of *Arabidopsis thaliana*. *Science* **301,** 653–657.

Balachandran S, Xiang Y, Schobert C, Thompsom GA, Lucas WJ. 1997. Phloem sap proteins from *Cucurbita maxima* and *Ricinus communis* have the capacity to traffic cell to cell through plasmodesmata. *Proceedings of the National Academy of Sciences, USA* **94,** 14150–14155.

Baunsgaard L, Lütken H, Mikkelsen R, Glaring MA, Pham TT, Blennow A. 2005. A novel isoform of glucan, water dikinase phosphorylates pre-phosphorylated α-glucans and is involved in starch degradation in *Arabidopsis*. *The Plant Journal* **41,** 595–605.

Behnke HD. 2003. Sieve-element plastids and evolution of monocotyledons, with emphasis on Melanthiaceae sensu lato and Aristolochiaceae-Asaroideae, a putative dicotyledon sister group. *Botanical Reviews* **68,** 524–544.

Blennow A, Bay-Smidt AM, Olsen CE, Møller BL. 1998. Analysis of starch bound glucose 3-phosphate and glucose 6-phosphate using controlled acid treatment combined with high-performance anion-exchange chromatography. *Journal of Chromatography A* **829,** 385–391.

Blennow A, Nielsen TH, Baunsgaard L, Mikkelsen R, Engelsen SB. 2002. Starch phosphorylation: a new front line in starch research. *Trends in Plant Science* **7,** 445–450.

Chia T, Thorneycroft D, Chapple A, Messerli G, Chen J, Zeeman SC, Smith SM, Smith AM. 2004. A cytosolic glucosyltransferase is required for conversion of starch to sucrose in *Arabidopsis* leaves at night. *The Plant Journal* **37,** 853–863.

Coppin A, Varré JS, Lienard L, Dauvillée D, Guérardel Y, Soyer-Gobillard MO, Buléon A, Ball S, Tomavo S. 2005. Evolution of plant-like crystalline storage polysaccharides in the protozoan parasite *Toxoplasma gondii* argues for a red alga ancestry. *Journal of Molecular Evolution* **60,** 257–267.

Delatte T, Umhang M, Trevisan M, Eicke S, Thorneycroft D, Smith SM, Zeeman SC. 2006. Evidence for distinct mechanisms of starch granule breakdown in plants. *Journal of Biological Chemistry* **281,** 12050–12059.

Edner C, Li J, Albrecht T, *et al.* 2007. Glucan, water dikinase activity stimulates breakdown of starch granules by plastidial β-amylases. *Plant Physiology* **145,** 17–28.

Emanuelsson O, Nielsen H, Brunak S, von Heijne G. 2000. Predicting subcellular localization of proteins based on their N-terminal amino acid sequence. *Journal of Molecular Biology* **300,** 1005–1016.

Fettke J, Chia T, Eckermann N, Smith A, Steup M. 2006. A transglucosidase necessary for starch degradation and maltose metabolism in leaves at night acts on cytosolic heteroglycans (SHG). *The Plant Journal* **46,** 668–684.

Fettke J, Eckermann N, Tiessen A, Geigenberger P, Steup M. 2005. Identification, subcellular localization and biochemical characterization of water-soluble heteroglycans (SHG) in leaves of *Arabidopsis thaliana* L.: distinct SHG reside in the cytosol and in the apoplast. *The Plant Journal* **43,** 568–585.

Haseloff J, Siemering KR, Prasher DC, Hodge S. 1997. Removal of a cryptic intron and subcellular localization of green fluorescent protein are required to mark transgenic *Arabidopsis* plants brightly. *Proceedings of the National Academy of Sciences, USA* **94,** 2122–2127.

Kaplan F, Guy CL. 2005. RNA interference of *Arabidopsis* beta-amylase8 prevents maltose accumulation upon cold shock and increases sensitivity of PSII photochemical efficiency to freezing stress. *The Plant Journal* **44,** 730–743.

Karimi M, Inzé D, Depicker A. 2002. GATEWAY™ vectors for *Agrobacterium*-mediated plant transformation. *Trends in Plant Science* **7,** 193–195.

Knoblauch M, van Bel AJE. 1998. Sieve tubes in action. *The Plant Cell* **10,** 35–50.

Kötting O, Pusch K, Tiessen A, Geigenberger P, Steup M, Ritte G. 2005. Identification of a novel enzyme required for starch metabolism in *Arabidopsis* leaves. The phosphoglucan, water dikinase. *Plant Physiology* **137,** 242–252.

Kühn C, Franceschi VR, Schulz A, Lemoine R, Frommer WB. 1997. Macromolecular trafficking indicated by localization and turnover of sucrose transporters in enucleate sieve elements. *Science* **275,** 1298–1300.

Kumar S, Tamura K, Nei M. 2004. MEGA3: Integrated software for molecular evolutionary genetics analysis and sequence alignment. *Briefings in Bioinformatics* **5,** 150–163.

Krysan PJ, Young JK, Sussman MR. 1999. T-DNA as an insertional mutagen in *Arabidopsis*. *The Plant Cell* **11,** 2283–2290.

Laby RJ, Kim D, Gibson SI. 2001. The *ram1* mutant of *Arabidopsis* exhibits severely decreased β-amylase activity. *Plant Physiology* **127,** 1798–1807.

Lee JY, Yoo BC, Rojas MR, Gomez-Ospina N, Staehelin LA, Lucas WJ. 2003. Selective trafficking of non-cell-autonomous proteins mediated by NtNCAPP1. *Science* **299,** 392–396.

Lloyd JR, Kossman J, Ritte G. 2005. Leaf starch degradation comes out of the shadows. *Trends in Plant Science* **10,** 130–137.

Lorberth R, Ritte G, Willmitzer L, Kossman J. 1998. Inhibition of a starch-granule-bound protein leads to modified starch and repression of cold sweetening. *Nature Biotechnology* **16,** 473–477.

Lough TJ, Lucas WJ. 2006. Integrative plant biology: role of phloem long-distance macromolecular trafficking. *Annual Review of Plant Biology* **57,** 203–232.

Lu Y, Sharkey TD. 2004. The role of amylomaltase in maltose metabolism in the cytosol of photosynthetic cells. *Planta* **218,** 466–473.

Mikkelsen R, Baunsgaard L, Blennow A. 2004. Functional characterization of α-glucan, water dikinase, the starch phosphorylating enzyme. *Biochemical Journal* **377,** 525–532.

Mikkelsen R, Suszkiewicz K, Blennow A. 2006. A novel type carbohydrate-binding module identified in α-glucan, water dikinase is specific for regulated plastidial starch metabolism. *Biochemistry* **45,** 4674–4682.

Mita S, Suzuki-Fujii K, Nakamura K. 1995. Sugar-inducible expression of a gene for β-amylase in *Arabidopsis thaliana*. *Plant Physiology* **107,** 895–904.

Nielsen TH, Wischmann B, Enevoldsen K, Møller BL. 1994. Starch phosphorylation in potato tubers proceeds concurrently with *de novo* biosynthesis of starch. *Plant Physiology* **105,** 111–117.

Niittylä T, Messerli G, Trevisan M, Chen J, Smith AM, Zeeman SC. 2004. A previously unknown maltose transporter essential for starch degradation in leaves. *Science* **303,** 87–89.

Nour-Eldin HH, Hansen BG, Nørholm MHH, Jensen JK, Halkier BA. 2006. Advancing uracil-excision based cloning towards an ideal technique for cloning PCR fragments. *Nucleic Acids Research* **34,** e122.

Palevitz BA, Newcomb EH. 1970. A study of sieve element starch using sequential enzymatic digestion and electron microscopy. *Journal of Cell Biology* **45,** 383–398.

Ral JP, Derelle E, Ferraz C, *et al.* 2004. Starch division and partitioning. A mechanism for granule propagation and maintenance

in the picophytoplanktonic green alga *Ostreococcus tauri*. *Plant Physiology* **136,** 1–8.

Ritte G, Heydenreich M, Mahlow S, Haebel S, Kötting O, Steup M. 2006. Phosphorylation of C6- and C3-positions of glycosyl residues in starch is catalysed by distinct dikinases. *FEBS Letters* **580,** 4872–4876.

Ritte G, Lloyd JR, Eckermann N, Rottmann A, Kossman J, Steup M. 2002. The starch-related R1 protein is an α-glucan, water dikinase. *Proceedings of the National Academy of Sciences, USA* **99,** 7166–7171.

Ritte G, Scharf A, Eckermann N, Haebel S, Steup M. 2004. Phosphorylation of transitory starch is increased during degradation. *Plant Physiology* **135,** 1–10.

Ritte G, Steup M, Kossman J, Lloyd JR. 2003. Determination of the starch-phosphorylating enzyme activity in plant extracts. *Planta* **216,** 798–801.

Robinson C, Mant A. 2002. Import of proteins into isolated chloroplasts and thylakoid membranes. In: Gilmartin PM, Bowler C, eds. *Molecular plant biology: a practical approach*, Vol. 2. Oxford, UK: Oxford University Press, 123–146.

Rosso MG, Li Y, Strizhov N, Reiss B, Dekker K, Weisshaar B. 2003. An *Arabidopsis thaliana* T-DNA mutagenized population (GABI-Kat) for flanking sequence tag-based reverse genetics. *Plant Molecular Biology* **53,** 247–259.

Small I, Peeters N, Legeai F, Lurin C. 2004. Predotar: a tool for rapidly screening proteomes for N-terminal targeting sequences. *Proteomics* **4,** 1581–1590.

Scheidig A, Fröhlich A, Schulze S, Lloyd JR, Kossman J. 2002. Downregulation of a chloroplast-targeted β-amylase leads to a starch-excess phenotype in leaves. *The Plant Journal* **30,** 581–591.

Schulz A, Kühn C, Riesmeier JW, Frommer WB. 1998. Ultrastructural effects in potato leaves due to antisense-inhibition of the sucrose transporter indicate an apoplasmic mode of phloem loading. *Planta* **206,** 533–543.

Smith AM, Zeeman SC, Smith SM. 2005. Starch degradation. *Annual Review of Plant Biology* **56,** 73–98.

van Bel AJE, Ehlers K, Knoblauch M. 2002. Sieve elements caught in the act. *Trends in Plant Science* **7,** 126–132.

Voinnet O, Rivas S, Mestre P, Baulcombe D. 2003. An enhanced transient expression system in plants based on suppression of gene silencing by the p19 protein of tomato bushy stunt virus. *The Plant Journal* **33,** 949–956.

Wang Q, Monroe J, Sjölund RD. 1995. Identification and characterization of a phloem-specific β-amylase. *Plant Physiology* **109,** 743–750.

Weise SE, Weber APM, Sharkey TD. 2004. Maltose is the major form of carbon exported from the chloroplast at night. *Planta* **218,** 474–482.

Wu H, Zheng XF. 2003. Ultrastructural studies on the sieve elements in root protophloem of *Arabidopsis thaliana*. *Acta Botanica Sinica* **45,** 322–330.

Yu TS, Kofler H, Häusler RE, *et al*. 2001. The *Arabidopsis sex1* mutant is defective in the R1 protein, a general regulator of starch degradation in plants, and not in the chloroplast hexose transporter. *The Plant Cell* **13,** 1907–1918.

Yu TS, Zeeman SC, Thorneycroft D, *et al*. 2005. α-amylase is not required for breakdown of transitory starch in *Arabidopsis* leaves. *Journal of Biological Chemistry* **280,** 9773–9779.

Zeeman SC, Smith SM, Smith AM. 2007. The diurnal metabolism of leaf starch. *Biochemical Journal* **401,** 13–28.

Zeeman SC, Thorneycroft D, Schupp N, Chapple A, Weck M, Dunstan H, Haldimann P, Bechtold N, Smith AM, Smith SM. 2004. Plastidial α-glucan phosphorylase is not required for starch degradation in *Arabidopsis* leaves but has a role in the tolerance of abiotic stress. *Plant Physiology* **135,** 1–10.

Zimmermann P, Hirsch-Hoffmann M, Hennig L, Gruissem W. 2004. GENEVESTIGATOR. *Arabidopsis* microarray database and analysis toolbox. *Plant Physiology* **136,** 2621–2632.